Approach and Landing Simulator for Space Shuttle Orbiter Touchdown Conditions

Keith D. Walyus*
NASA Johnson Space Center, Houston, Texas 77058
and
Charles Dalton†
University of Houston, Houston, Texas 77204

This study describes a computer simulation that provides an accurate calculation of the touchdown conditions. The program is small enough to operate on a personal computer. The program simulates the Orbiter trajectory from an altitude of 10,000 ft to the Earth's surface. It assumes the Orbiter flies close to its reference altitude profile, with negligible crosswind effects. Flight data have proven both assumptions to be valid. By incorporating these assumptions with the Shuttle guidance logic, a quick approximation can be made of the touchdown speed and downrange distance to an accuracy within 400 ft of the mainframe prediction.

Nomenclature

C_D = vehicle drag coefficient
C_{Db} = basic, full-scale, freestream body C_D
C_{Dbf} = change in C_D due to the body flap
C_{De} = change in C_D due to elevons
C_{Dge} = change in C_D due to the ground effects
C_{Dlg} = change in C_D due to the landing gear
C_{Dsb} = change in C_D due to the speedbrake
C_{Dref} = C_D corresponding to reference speedbrake position
C_D/SB = $C_{\dot{D}}$ to speedbrake deflection ratio
D = ground relative drag
D_∞ = drag relative to the freestreem
F = total aerodynamic force on the vehicle
g = gravitational constants, = 32.174 ft/s^2
h = vehicle altitude
$\dot{h}$ = vehicle altitude rate
K_{sb} = speedbrake control constant, = 2 deg × s/ft
K_{sbi} = speedbrake integral multiplicative constant, = 0.1 deg/ft
L = ground relative lift
L_∞ = freestream lift force
m = mass of the vehicle
q_∞ = dynamic pressure
S = vehicle wing area, = 2690 ft^2
$SBDEF$ = commanded speedbrake deflection
SB_{ref} = reference speedbrake position, = 65 deg
S_{bi} = integral multiplicative factor
V = ground relative velocity
V_{eas} = equivalent airspeed
V_{error} = equivalent airspeed error, = V_{eas} − 490
V_∞ = freestream Orbiter velocity at altitude
$\dot{V}$ = ground relative deceleration
V_2 = updated ground relative velocity
V_w = velocity of the wind
β = constant for air density calculation
Γ = landing gear deployment angle
γ = ground relative flight-path angle
$\dot{\gamma}$ = ground relative flight-path angle rate
γ_∞ = freestream flight-path angle
ΔS = vehicle displacement
Δt = time step
Θ = vehicle pitch angle
ρ_a = air density of the freestream at altitude
ρ_o = air density at sea level for 62 standard atmosphere
Φ = angle between the relative drag and the total aerodynamic force on the vehicle

Received July 2, 1990; revision received and accepted for publication Nov. 30, 1990. Copyright © 1991 by the American Institute of Aeronautics and Astronautics, Inc. No copyright is asserted in the United States under Title 17, U.S. Code. The U.S. Government has a royalty-free license to exercise all rights under the copyright claimed herein for Governmental purposes. All other rights are reserved by the copyright owner.

*Descent Flight Design Engineer. Member AIAA.
†Professor of Mechanical Engineering, Department of Mechanical Engineering. Associate Fellow AIAA.

I. Introduction

SINCE the Space Shuttle Orbiter does not use its engines while landing, the Shuttle commander requires an accurate prediction of the Orbiter touchdown speed and downrange distance to ensure a safe landing and rollout on the runway. The Orbiter is essentially a glider and does not have any thrust capability to aid in the landing. Without engines, the Orbiter has no go-around capability and cannot use thrust to modulate its airspeed. If the vehicle energy is too high, it may run off the end of the runway, whereas, if the energy is too low, it may undershoot the runway. The nominal landing site at Edwards Air Force Base in California is a smoothed lake bed with ample under-run and over-run distance to protect for contingency situations. However, some emergency sites have much shorter runways that require very strict control of the Orbiter touchdown speed and downrange distance. Landing short or rolling off the runway could be disastrous, considering that the land at these sites may consist of desert, swampland, or other hazardous terrains.

The commander does have the capability to change the approach geometry and computer guidance logic to present the most favorable conditions for landing. These geometry and guidance changes are based on recommendations from flight controllers in the Mission Control Center (MCC). The MCC will radio this information to the crew prior to the deorbit burn and update the information if necessary during the entry. Prior to the landing approach, landing analysts receive atmospheric data from weather balloons, plane reports, and surface observations. They then examine the data using various computer tools that enable them to make recommendations on the approach geometry and guidance logic that the crew will use. The most important of these tools is the Autoland Shaping Processor (ASP), which is hosted on the mainframe UNIVAC 1192S computer. This processor is a three-degree-

of-freedom simulation in range to runway, vehicle altitude, and vehicle pitch attitude. It uses the Orbiter guidance logic to predict the Orbiter touchdown speed and downrange distance. The ASP assumes that the crosswind effects are negligible and that the Orbiter is in line with the runway plane. These assumptions allow the three-degree-of-freedom processor to provide accuracy comparable to that of a six-degree-of-freedom simulation. The ASP also assumes that the autoland guidance system, and not the commander, is flying the vehicle. Examination of postflight data and prelanding predictions has proven the validity of these assumptions. Although all commanders have flown the vehicle to touchdown, the differences between the autoland-flown profile and the pilot-flown profiles have usually been small. The commander also uses guidance commands as an aid, since his heads-up display is driven by autoland guidance, even when autoland guidance is not actively flying the vehicle.

One limitation on the ASP is its computation speed. Calculations of a single approach profile can take up to 1 min. If the Orbiter is still in orbit and the approach profile is still being planned, a 1 min computation time will suffice. If the Orbiter has already entered the atmosphere and the wind shifts or a system failure dictates a change in the approach profile, the ASP may not be sufficiently responsive. Also, slow response time may limit the ASP from analyzing potential emergency landing sites during a launch abort. Ideally, a simulation is needed that provides a quicker execution time without a significant loss in accuracy.

This paper describes such a simulation, called the Approach and Landing Predictor (ALP). The ALP is a quick-look simulation designed to provide a touchdown energy accurate to within 400 ft of the ASP simulation, where the touchdown energy is defined as the touchdown velocity and downrange distance on the runway. It will calculate the touchdown energy for all vehicle weights and under all expected density altitudes. The density altitude represents the altitude at which the U.S. 62 Standard Atmosphere has the same density as the surface density of the landing site.[1] Although the ASP uses density calculations based on balloon data when available, the ALP will only use the density altitude approximations, which usually provide an adequate approximation to the atmospheric density profile. During mission support the ASP receives wind and atmospheric data from weather balloons launched at potential landing sites. The data arrives in 500- or 1,000- ft increments, and the ASP interpolates to calculate in-between values. Since the touchdown energy is very sensitive to the wind profile, the ALP, like the ASP, will use weather balloon information from the landing site to model the wind profile.

Another use for the ALP will be under contingency situations. If the MCC in Houston was forced to close during a mission, an Emergency Mission Control Center (EMCC) would be established at White Sands, New Mexico. A team of flight controllers would fly to New Mexico, where communications would be re-established. Unfortunately, the computer hardware necessary to run the ASP could not follow the EMCC team to New Mexico. The ALP, however, can be stored on a single low-density floppy disk. Since it is written in ASCII FORTRAN, the program is portable and can be used easily by most computers. The new ALP will give the EMCC team a valid computer simulation despite being cut off from the MCC back in Houston.

II. Background

The Orbiter descent trajectory is divided into three different guidance phases, the final phase of which is called the approach and landing phase. The approach and landing phase typically begins at an altitude of 10,000 ft with a range from the runway of 7–8 nm (Fig. 1).

Shortly before the approach and landing phase begins, the Orbiter lines up on the runway centerline and begins to descend along a constant glideslope. Vehicles weighing >220,000 lb usually use a 17-deg glideslope, whereas vehicles weighing <220,000 lb usually use a 19-deg glideslope. Using a shallow glideslope for heavy vehicles allows the speedbrake (Fig. 2) to control the vehicle velocity in the presence of atmospheric dispersions without becoming saturated. The 19-deg glideslope provides sufficient speedbrake control for lightweight vehicles.

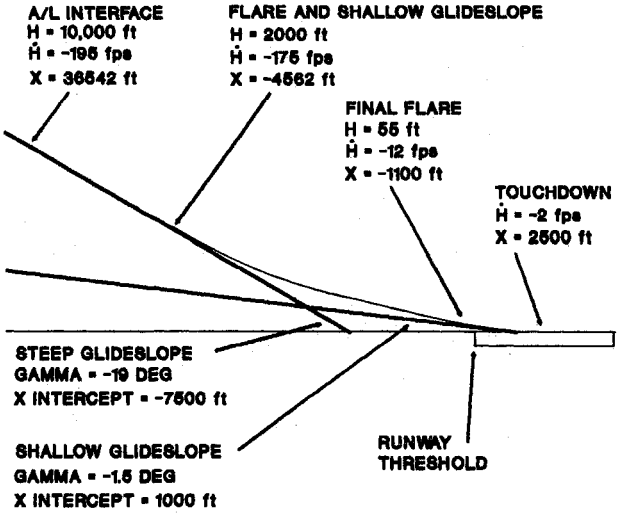

Fig. 1 Approach and landing geometry overview.

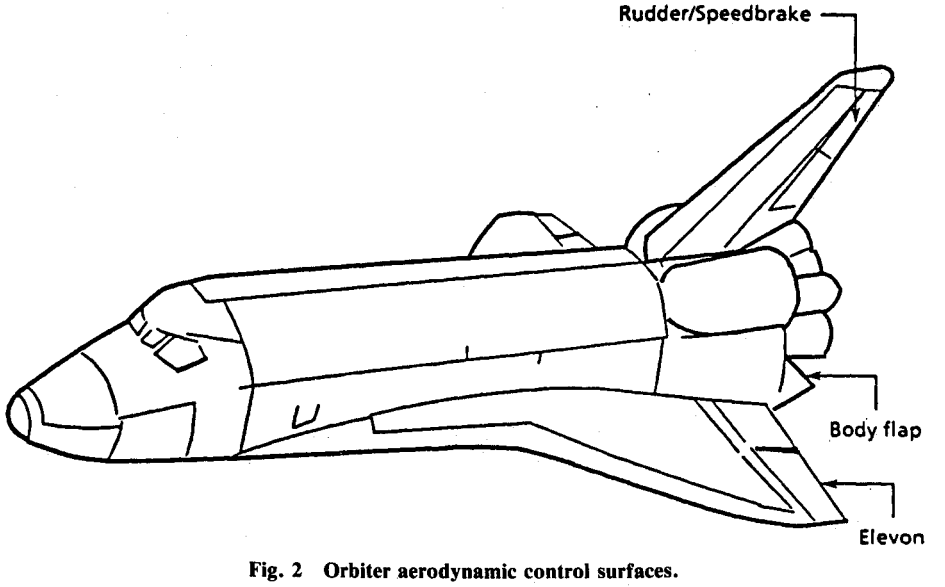

Fig. 2 Orbiter aerodynamic control surfaces.

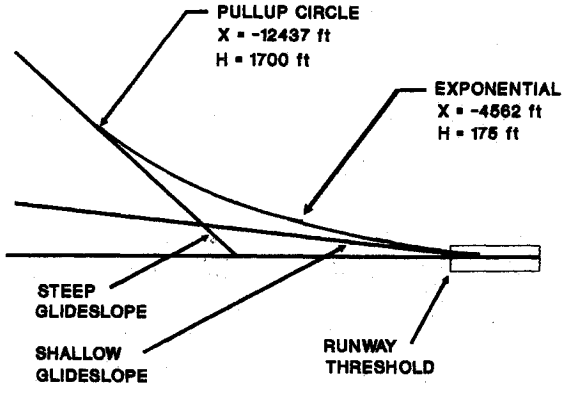

Fig. 3 Flare geometry.

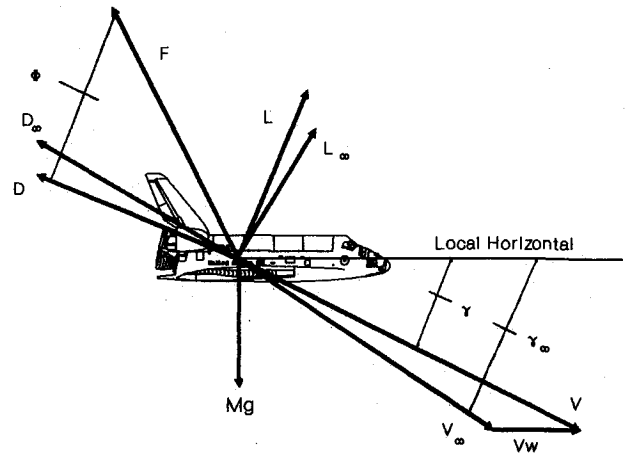

Fig. 4 Relative and freestream force relationship.

Both glideslopes intersect the ground 7500 ft before the runway threshold, with the ground intersection acting as the commander's aim point. However, conditions may cause the vehicle energy state to be too low when approaching the runway to eliminate landing dispersions. A vehicle flying into a strong headwind will require more energy than a vehicle flying into a more benign wind. For this scenario, the Orbiter flies the same glideslope, but the aim point is located 6500 ft from the runway threshold instead of 7500 ft. This aim point shift will effectively give the Orbiter 1000 ft more of touchdown energy. To date, 12 flights have used the close-in aim points, with 21 using nominal aim points.

The ASP simulates a guidance-flown trajectory during the approach and landing phase of the descent. The ASP has the capability to initiate a simulation at a nominal altitude of 10,000 ft or lower. Since it is a quick-look simulation, the ALP will be restricted to beginning its simulation at 10,000 ft by assuming that errors to the cross range, range, flight-path angle, and dynamic pressure are zero. This is a valid assumption because the pilot follows guidance commands and usually corrects most trajectory errors prior to the Orbiter reaching 10,000 ft. Approach and landing guidance commands are computed through touchdown, and parts of approach and landing guidance will remain active during the rollout.

At an altitude of 10,000 ft, guidance begins using the speedbrake to control the airspeed to a reference velocity of 490 fps equivalent airspeed. Equivalent airspeed is defined as

$$\tfrac{1}{2}\rho_a V_\infty^2 = \tfrac{1}{2}\rho_o V_{eas}^2 = q_\infty \qquad (1)$$

or

$$V_{eas} = \sqrt{(2/\rho_o)}\sqrt{q_\infty} \qquad (2)$$

By having a constant equivalent airspeed, the vehicle maintains a constant dynamic pressure despite changing air densities and surface winds.

Below 3000 ft, the vehicle performs a series of flares that will arrest its altitude descent rate from 180 to 2 fps at touchdown (Fig. 1). At 3000 ft, guidance stops controlling the airspeed and retracts the speedbrake to a set position. Freezing the speedbrake position keeps the aerosurface movement to a minimum, yet still gives the Orbiter the necessary energy required to land safely. The speedbrake retraction position is based on six factors: the winds of the day, the density altitude of the day, the vehicle weight, equivalent airspeed error at 3000 ft, the glideslope that was chosen, and whether the speedbrake is following nominal or short-field guidance. Short-field guidance is used when the vehicle has high energy and may experience stopping or braking problems. It will most commonly be used at emergency sites where the runways are shorter. The speedbrake position is updated once more at 500 ft and reflects the changes in the wind profile and density altitude encountered since the initial retraction at 3000 ft.

At 1800 ft, the vehicle leaves the outer glideslope. It then performs a flare onto a shallower glideslope of 1.5 deg and reduces the altitude rate to 12 fps. During this first flare, the vehicle follows a circular trajectory, which then exponentially transitions onto the shallow glideslope (Fig. 3). The second flare reduces the altitude rate on the shallow glideslope to a safe value at touchdown.

III. Methods

The ALP computer simulation is composed essentially of two parts. The first part models flight on the outer glideslope while the speedbrake controls the vehicle velocity. At an altitude of 3000 ft, the speedbrake stops controlling the velocity and retracts to a set position. The second part of the ALP models the flight from 3000 ft to the surface.

A. Flight Above 3000 Feet

While on the outer glideslope, autoland guidance follows reference-altitude and altitude-rate profiles. Altitude errors, altitude-rate errors, and the integral of the altitude errors are converted into normal acceleration commands. The flight control system then converts the normal acceleration commands into surface deflections for the elevons.

Being a full three-degree-of-freedom simulation, the ASP calculates the vehicle velocity error and altitude error from the reference profile. Conversely, the ALP disregards altitude errors and assumes that the vehicle always stays on the reference glideslope. This is a valid assumption, due to the Orbiter ability to maintain the reference altitude even in the presence of strong wind shears. The largest wind shear on the outer glideslope to date was seen on flight STS-3, which flew during March of 1982. The STS-3 wind had a 15-kt/1000 foot wind shear, which occurred over a 1000-ft span, followed by a shear of 10 kt/1000 ft. Even in the presence of these two shears, the resulting altitude error never exceeded 20 ft. This small altitude error in the presence of large wind shears demonstrates the validity of assuming that the vehicle remains on the reference guidepath at all times.

Between 10,000 and 3000 ft, the vehicle uses its speedbrake to control its velocity to a reference 490 fps of equivalent airspeed. The speedbrake command to guidance is composed of three terms[2]:

$$SBDEF = SB_{ref} + K_{sb} V_{error} + K_{sbi}(\Sigma V_{error}/\Delta t) \qquad (3)$$

The first two terms on the right side of the equation model a first-order transfer function with the velocity measured in equivalent airspeed. The velocity error does not damp to the reference velocity of 490 fps but rather approaches a standoff velocity near 490 fps with time. The third term corrects for the

standoff error and will bring the Orbiter velocity back to the reference velocity over a period of time.

By assuming an exponential relation for the air density and using the equations of motion, it can be shown that a given drag coefficient C_D is required to maintain a constant equivalent airspeed. As was shown in Eq. (2), a vehicle flying a constant equivalent airspeed will maintain a constant dynamic pressure and, therefore, gives

$$\dot{q}_\infty = 0 = \tfrac{1}{2}(\dot{\rho}_a V_\infty^2 + 2\rho_a V_\infty \dot{V}_\infty) \tag{4}$$

Using an exponential relationship for the air density of

$$\dot{\rho}_a = \rho_o \exp(-\beta h) \tag{5}$$

and taking its derivative with respect to time yields

$$\dot{\rho}_a = -\beta \rho_a \dot{h} \tag{6}$$

or

$$\dot{\rho}_a = -\beta \rho_a V \sin(\gamma) \tag{7}$$

From the vehicle force diagram (Fig. 4), we get the deceleration equation for the vehicle,

$$-\dot{V}_\infty = [D_\infty/m] + g \sin(\gamma_\infty) \tag{8}$$

or

$$\dot{V}_\infty = -(\tfrac{1}{2}\rho_a V_\infty^2 S C_D/m) - g \sin(\gamma_\infty) \tag{9}$$

Combining Eqs. (4), (7), and (9) yields

$$C_D = -m[\beta V \sin(\gamma) - 2g \sin(\gamma_\infty)/V_\infty]/(\rho_a V_\infty^2 s) \tag{10}$$

The velocities V and V_∞ are depicted in Fig. 4 and are described by

$$V = [V_\infty \cos(\gamma_\infty) - V_w]/\cos(\gamma) \tag{11}$$

Equation (10) shows the relation between atmospheric conditions, the vehicle weight, and the drag coefficient required to maintain a constant dynamic pressure. Clearly, a change in any of the terms on the right side of Eq. (10) will require a corresponding change in C_D if a constant equivalent airspeed is to be maintained.

The standoff error in equivalent airspeed arises from the speedbrake attempting to control the velocity of different weight vehicles while flying through various densities with different wind velocities. For each 1 fps of positive velocity error, the speedbrake opens 2 deg, regardless of the vehicle weight or atmospheric conditions. The resultant change in the vehicle drag coefficient will always be the same, but the impact on the deceleration of the vehicle will vary. Figure 5 shows the sensitivity of the standoff velocity to vehicle weight, with the integral constant being set to zero.

On the outer glideslope, the Orbiter angle of attack changes only slightly, leaving the speedbrake as the primary controller of C_D. Modifying Eq. (3) to reflect this yields

$$C_D = C_{D\text{ref}} + (C_D/\text{SB}) K_{\text{sb}} V_{\text{error}} \tag{12}$$

The C_D/SB ratio represents a least-squares fit of the effect of the speedbrake on the coefficient of drag. The least-squares fit was determined from Orbiter aerodynamic data.[3]

By comparing C_D in Eq. (10) with C_D in Eq. (12), and by iterating on the freestream velocity, we can find the freestream velocity, which causes the equations to be equal. Equation (10) contains the freestream velocity term explicitly, whereas the velocity error in Eq. (12) has the freestream velocity embedded in it.

Because the ALP does not simulate the guidance and flight control systems exactly, different values must be employed for the constants in the equations as opposed to those used onboard by the Orbiter. Two terms, the speedbrake control constant and the speedbrake integral multiplicative constant, were developed empirically based on ASP simulations. Using the method just mentioned to calculate the velocity, and assuming that the vehicle flies along the reference glideslope, a six-step method for computing the trajectory along the outer glideslope can be developed:

1) Calculate the change in wind speed and air density from the previous altitude.

2) Iteratively calculate the new standoff velocity error with the freestream velocity used as the iterative variable.

3) Compute the total velocity error. The total velocity error consists of two terms, the standoff velocity error and any velocity error due to a wind shear. The two terms are modeled by first-order linear transfer functions and are summed with previous terms.

4) The final velocity offset from the reference equivalent airspeed is computed by adding the integral effects to the velocity error.

5) Convert the equivalent airspeed into a freestream velocity and finally into a ground speed.

6) Move the Orbiter along the glideslope, and repeat this process until the Orbiter descends to 3000 ft.

For this method to remain valid, the speedbrake must not reach its lower 15-deg or upper 100-deg limit. If it does, the transfer functions will be invalid due to the inability of the speedbrake to correct the velocity error. This is not an overly restrictive condition, because only a few of the flights have required the speedbrake to reach its limits on the outer glideslope. Still, it will be safer to restrict the program to situations where the speedbrake is not limited, which should only have a minor impact on its use.

To incorporate this restriction, the program must have the ability to predict when the speedbrake has reached its limits. By using Eq. (3), the speedbrake position can be calculated and a warning will be displayed stating that the results may be inaccurate due to the speedbrake being limited.

B. Flight Below 3000 Feet

At 3000 ft, the speedbrake retracts to a calculated position, which is estimated to give the Orbiter the energy required to achieve a touchdown distance of 2500 ft with an equivalent airspeed of 195 kt. As previously mentioned, the speedbrake retraction logic is based on six factors: wind speed, density altitude, vehicle weight, velocity error from the reference at 3000 ft, aim-point choice, and whether short-field speedbrake guidance is being employed. Both short-field guidance and use of close-in aim-points add 11–12 deg to the speedbrake angle. For the other four parameters, speedbrake sensitivities to downrange distance have been incorporated into the speedbrake calculation.

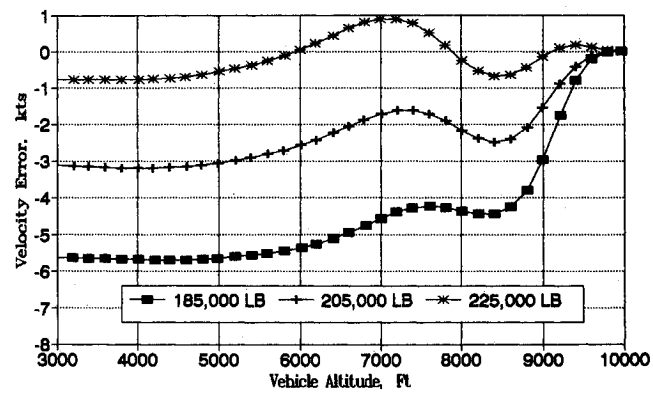

Fig. 5 Standoff velocity sensitivity to vehicle weight.

At 500 ft, the speedbrake position is updated based on any changes in the wind speed and density altitude. Also, the maximum deflection allowed for nominal speedbrake guidance is now restricted to 50 deg. Higher speedbrake settings will decrease the lift-to-drag ratio and make handling more difficult. Short-field speedbrake guidance does allow the speedbrake to open more than 50 deg. This guidance mode would only be employed if the vehicle had stopping or braking problems where reducing the downrange distance is important. Hardware limits dictate a 15-deg minimum setting for the speedbrake for all guidance modes.

Because the Orbiter only uses pressure probes, it must use pressure tables to calculate its true airspeed. The pressure tables are based on the U.S. 62 Standard Atmosphere with seasonal corrections. Like the Orbiter, the ALP and the ASP both modify their true airspeed calculations to compensate for the seasonal temperature adjustments. From the true airspeed and equivalent airspeed, the density altitude and wind speed for the speedbrake are calculated.

As before, guidance commands the Orbiter to follow reference-altitude and altitude-rate profiles. However, the profile is no longer simply along a constant glideslope. From 3000 ft down to 1800 ft, the vehicle still follows the outer glideslope. At 1800 ft, the vehicle initiates the first of two flares, which will decrease the current altitude rate of 180 fps. The first flare follows a large circle (Fig. 3). Near the base of the circle, the profile exponentially decays onto a shallow glideslope of 1.5 deg.

Between 30 and 80 ft, guidance stops following a reference-altitude profile and switches solely to an altitude-rate profile. During this phase, the vehicle performs the final flare, which decreases the altitude descent rate from 12 fps to a safe rate at touchdown of 2 fps. The transition to an altitude-rate profile typically occurs near 55 ft, but if the vehicle has higher than normal energy, the transition may occur sooner. Conversely, vehicles with lower energy will transition later.

The ALP still assumes that the vehicle flies along the reference-altitude profile even in the presence of strong wind shears. However, since the vehicle is no longer controlling its energy with its speedbrake, a different scheme for modeling the flight is employed. For flight below 3000 ft, the equations of motion for an airplane will be used to calculate the velocity of the vehicle, with the displacement following along the reference-altitude profile.

The force diagram for the vehicle is shown in Fig. 4, with the equations of motion for the airplane being

$$mV\dot{\gamma} = L - g\cos(\gamma) \tag{13}$$

and

$$m\dot{V} = -D - g\sin(\gamma) \tag{14}$$

By assuming that the vehicle follows the reference-altitude profile, the relative flight-path angle and its first derivative are calculated easily. The ground relative lift L can be determined explicitly since all other terms in Eq. (13) are known. Equation (14), though, has two unknowns, the ground relative drag D and the deceleration $\dot{V}$. The deceleration is required to calculate the new velocity and displacement, but first the ground relative drag must be calculated. The standard equation for drag is

$$D_\infty = \tfrac{1}{2}\rho_a V_\infty^2 S C_D \tag{15}$$

This drag, however, represents the freestream drag and is not equivalent to the ground relative drag unless the wind velocity is zero. Figure 4 shows the relation between freestream aerodynamic forces and ground relative aerodynamic forces. By using this relationship, the ground relative drag can be calculated once the freestream forces are known.

To calculate the freestream forces, the freestream velocity and flight-path angle must first be calculated. Using Fig. 4 as a basis, we get

$$V_\infty = \sqrt{[V^2 + V_w^2 - 2VV_w\cos(180 - \gamma)]} \tag{16}$$

The coefficient of drag of the Orbiter is primarily a function of the following parameters[3]

$$C_D = C_{Db} + C_{De} + C_{Dbf} + C_{Dsb} + C_{Dlg} + C_{Dge} \tag{17}$$

The first four terms on the right side of Eq. (17) relate the aerosurfaces and the angle of attack to the drag coefficient. During the final 3000 ft of the descent, the body flap does not move at all and the elevons change position only slightly. By temporarily removing the landing gear effects and ground effects, the drag coefficient essentially becomes a function of the angle of attack and the speedbrake setting. By performing a regression analysis on a series of ASP simulation data, a polynomial expression can be found for the C_D calculation with C_D a function of the speedbrake setting and the angle of attack. The functional description for the drag coefficient is given by

$$C_D = f(\alpha, \mathrm{SB}) \tag{18}$$

The data for the equation are based on a series of ASP simulations. The simulations cover the entire weight, density altitude, and wind magnitude ranges that are expected to be experienced by the Orbiter. With the drag coefficient, the freestream drag can now be calculated and, again using Fig. 4, three equations can be derived that relate the freestream forces and the relative forces:

$$F^2 = L_\infty^2 + D_\infty^2 \tag{19}$$

$$F = L/\sin(\Phi) \tag{20}$$

$$\Phi = \arctan(L_\infty/D_\infty) + (\gamma - \gamma_\infty) \tag{21}$$

Combining Eqs. (13) and (19–21) yields an implicit equation for the freestream lift, which can be determined iteratively by

$$0 = \sqrt{\{[L/\sin(\arctan(L_\infty/D_\infty) + (\gamma - \gamma_\infty))]^2 - D_\infty^2\}} - L_\infty \tag{22}$$

With L_∞ known, Eq. (21) can be solved for Φ and Eq. (20) for F. With these two quantities, the ground relative drag can be calculated from

$$D = F_\infty\cos\Phi \tag{23}$$

which, when inserted into Eq. (14), yields the deceleration. The new velocity and the vehicle displacement can now be calculated from

$$V_2 = V + \dot{V}\Delta t \tag{24}$$

and

$$\Delta S = \tfrac{1}{2}(V_2 + V)\Delta t \tag{25}$$

The displacement will follow the reference-altitude profile for the outer glideslope, circularization, and exponential decay periods of the flight. On the outer glideslope, the vehicle will fly straight along the constant glideslope. During circularization, the distance ΔS will correspond to the arc length of the circle. Flight along the exponential path will be calculated using Romberg integration[4] along a curve.

During the final flare phase, guidance follows a linear altitude-rate vs altitude profile. With the velocity being

calculated from Eq. (24), and the reference-altitude rate known, the horizontal velocity and displacement can be found once the ground relative flight-path angle is known. During the exponential and final flare phases of the flight, the relative flight-path angle can be calculated from

$$\gamma = \sin(\dot{h}/V) \tag{26}$$

Finally, the angle of attack must be updated. The coefficient of lift can be found from

$$C_L = L_\infty/(\tfrac{1}{2}\rho_a V_\infty^2 S) \tag{27}$$

and the angle of attack can be computed from a polynomial equation as a function of the speedbrake setting and the coefficient of lift,

$$\alpha = f(C_L, \mathrm{SB}) \tag{28}$$

Not included in any of the polynomial equations for the drag coefficient or the angle of attack are the ground effect and landing-gear-effect terms. The effect on C_L and C_D of these two terms can be modeled easily from aerodynamic data.[3]

Nominally, the landing gear will be deployed at an altitude of 300 ft and will be fully deployed 6 s later. The landing gear effects are primarily a function of the deploy angle Γ and vary only slightly over the expected angle-of-attack range. Two equations were developed: Eq. (29) models the gear during deployment, and Eq. (30) models the gear once it is fully deployed. The gear is assumed to deploy at a constant rate of 16 deg/s, and is functionally described by

During deployment:

$$C_{Llg} = f(\Gamma) \tag{29}$$

After deployment:

$$C_{Llg} = f(\alpha) \tag{30}$$

Similar equations were developed for C_D.

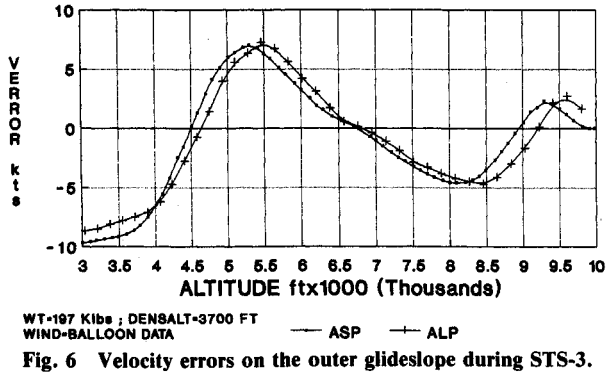

Fig. 6 Velocity errors on the outer glideslope during STS-3.

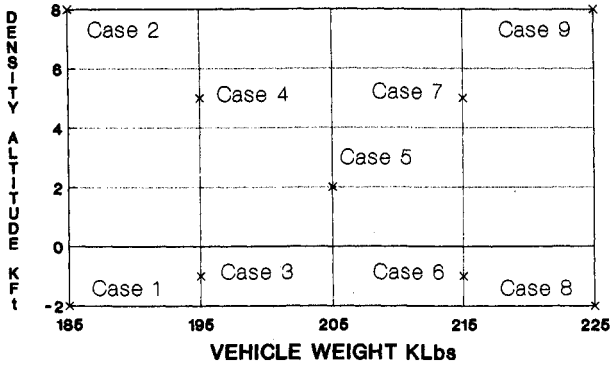

Fig. 7 Weight density altitude test matrix.

Ground effects play a significant role in arresting the Orbiter altitude rate near touchdown. The ground effects start to affect the Orbiter at an altitude of 80 ft and grow exponentially. At touchdown, ground effects will increase the Orbiter lift-over-drag ratio by approximately 25%. Ground effects are a function not only of the vehicle altitude and angle of attack, but also are a function of the elevon deflection. Since the elevons only deviate slightly near touchdown, a constant elevon deflection can be assumed, with the ground effects calculated as a function of the angle of attack and altitude. The equation can be functionally described by

$$C_{Lge} = f(\alpha, h) \tag{31}$$

The algorithm for flight below 3000 ft can now be summarized in nine steps:

1) Retract the speedbrake until it reaches its commanded value. The commanded value is a function of the wind speed, density altitude, vehicle weight, velocity error at 3000 ft, aimpoint selection, and guidance mode. The speedbrake position remains fixed until the vehicle descends to 500 ft, when a small update will be calculated due to changes in the winds and density altitude.
2) Calculate the new wind velocity and air density.
3) Calculate the new freestream velocity and flight-path angle.
4) Determine the new drag coefficient from the polynomial equation.
5) Calculate the freestream drag and the ground relative lift.
6) Iteratively calculate the freestream lift, which yields the angle Φ, and the ground relative drag.
7) Calculate the deceleration, the new vehicle velocity, and the vehicle displacement.
8) Move the vehicle along the reference-altitude profile or altitude-rate profile as the guidance phase dictates.
9) Calculate the new coefficient of lift and use the polynomial equation to determine the new angle of attack. For both C_L and C_D, the ground effects and landing gear effects are added at the appropriate altitudes.

IV. Results and Discussion

The results for flight above and below 3000 ft will be discussed separately. The same two-step methodology was used for both parts: first, develop equations that model the phase of flight, and then adjust the equations as required to correspond to ASP simulations.

The algorithm presented in the following will only describe vehicles flying on the 19-deg glideslope using nominal aim points and nominal speedbrake guidance. The same logic, though, can be applied to an orbiter flying any glideslope, aim point, or speedbrake guidance combination.

A. Flight Above 3000 Feet

The largest wind shear encountered on the outer glideslope occurred on STS-3 when the vehicle flew through a 15-kt/1000-ft wind shear followed by a reversing 10-kt/1000-ft wind shear. Figure 6 shows a comparison of the velocity error from the reference airspeed, between the ALP and the ASP, when STS-3 winds are used.

To guarantee the accuracy of the ALP under all expected conditions, a test matrix of weight and density altitudes was developed (Fig. 7). Nine test points were used to cover the field. The weight range covers all of the vehicle weights used in conjunction with a 19-deg glideslope. The density altitudes cover all expected density altitudes, with 8000 ft being a three standard-deviations hot day at Northrup Strip in New Mexico, and -2000 ft representing a three standard-deviations cold day at Kennedy Space Center in Florida.

Each point in Fig. 7 was tested to compare the velocity error between the ALP and the ASP. The wind profile for the test

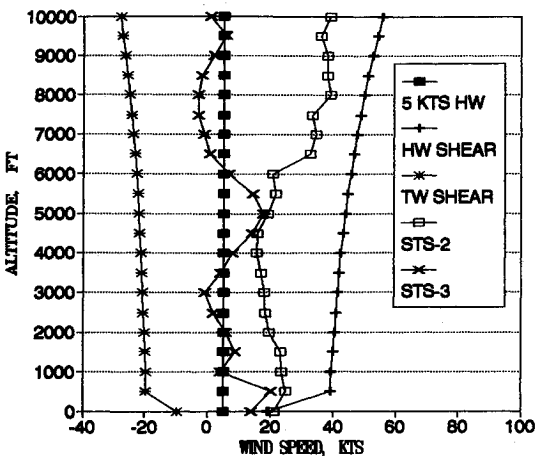

Fig. 8 Wind profiles used for verification below 3000 ft.

Table 1 Comparison of touchdown energies for Approach Landing Predictor vs Autoland Shaping Processor

Wind description	Case	Downrange distance, ft ASP	ALP	Difference
Design head-wind shear	1	−1810	−1916	106
	2	28	−97	125
	3	−1410	−1541	131
	4	−356	−472	116
	5	−630	−783	153
	6	−914	−1055	141
	7	260	365	−105
	8	−867	−1005	138
	9	1347	1588	−241
Design tail-wind shear	1	2304	2123	181
	2	3328	3204	124
	3	2500	2480	20
	4	2928	2859	69
	5	2747	2688	59
	6	2582	2534	48
	7	2906	2748	158
	8	2598	2561	37
	9	3468	3628	−160
STS-3 wind profile	1	656	335	321
	2	2952	2859	93
	3	1284	1050	234
	4	2611	2612	−1
	5	2353	2344	9
	6	2116	2067	49
	7	3382	3548	−166
	8	2251	2233	18
	9	4019	4403	−384
STS-2 wind profile	1	37	362	−325
	2	2430	2286	144
	3	639	338	301
	4	2046	1965	81
	5	1688	1597	91
	6	1362	1231	149
	7	2881	2945	−64
	8	1446	1266	180
	9	3920	4061	−141
5-kt steady head wind	1	673	414	259
	2	2987	2976	11
	3	1271	1088	183
	4	2559	2671	−112
	5	2272	2339	−67
	6	2022	2055	−33
	7	2972	3221	−249
	8	2122	2138	−16
	9	3585	3771	−186

Table 2 Comparison of 3000-ft speedbrake retraction position for Approach Landing Predictor vs Autoland Shaping Processor

Wind description	Case	Downrange distance, ft ASP	ALP	Difference
Design head-wind shear	1	14.8	14.8	0.0
	2	14.8	14.8	0.0
	3	14.8	14.8	0.0
	4	14.8	14.8	0.0
	5	14.8	14.8	0.0
	6	14.8	14.8	0.0
	7	14.8	14.8	0.0
	8	14.8	14.8	0.0
	9	14.8	14.8	0.0
Design tail-wind shear	1	17.7	17.4	0.3
	2	33.5	35.0	−1.5
	3	25.7	25.7	0.0
	4	35.2	36.9	−1.7
	5	35.4	36.9	−1.5
	6	35.6	36.1	−0.5
	7	45.2	47.4	−2.2
	8	37.7	38.3	−0.6
	9	54.1	56.2	−2.1
STS-3 wind profile	1	14.8	14.8	0.0
	2	14.8	14.8	0.0
	3	14.8	14.8	0.0
	4	14.8	14.8	0.0
	5	14.8	14.8	0.0
	6	14.8	14.8	0.0
	7	17.8	16.1	1.7
	8	14.8	14.8	0.0
	9	28.5	25.5	3.0
STS-2 wind profile	1	14.8	14.8	0.0
	2	14.8	14.8	0.0
	3	14.8	14.8	0.0
	4	14.8	14.8	0.0
	5	14.8	14.8	0.0
	6	14.8	14.8	0.0
	7	14.8	14.8	0.0
	8	14.8	14.8	0.0
	9	21.5	22.2	−0.7
5-kt steady head wind	1	14.8	14.9	0.0
	2	14.8	14.8	0.0
	3	14.8	14.8	0.0
	4	14.8	14.8	0.0
	5	14.8	14.8	0.0
	6	14.8	14.8	0.0
	7	21.3	23.0	−1.7
	8	14.8	14.8	0.0
	9	29.7	31.9	−2.2

matrix consisted of two 15-kt/1000-ft wind shears, which is slightly more severe than the profile experienced on STS-3. For all cases, the velocity error between the ALP and the ASP remained within an acceptable ±4 kt.

An accurate velocity calculation is very important on the outer glideslope, since the velocity must be passed on to the second half of the simulation at 3000 ft. Also, the velocity error at 3000 ft is a component of the speedbrake retraction position.

B. Flight Below 3000 Feet

Although the touchdown velocity of the vehicle will vary with the vehicle weight and the atmospheric conditions of the day, all touchdown energies are normalized to a standard touchdown equivalent airspeed of 195 kt. Normalization gives analysts a standard by which to judge the energy of the vehicle and also facilitates, in writing, flight rules for the landing.

After the final flare, the equivalent airspeed of the Orbiter changes linearly with downrange distance. This relationship allows the use of a linear least-squares fit to approximate the

downrange touchdown distance for an equivalent airspeed of 195 kt.

The test matrix below 3000 ft will use the same density altitude and weight pairs as in Fig. 7, but five different wind profiles will be used to test the nine points (Fig. 8). The first wind profile has a steady 5-kt head wind, which is close to the average touchdown head wind encountered on the 30 Space Shuttle landings. The second and third profiles are head-wind and tail-wind shearing profiles. The tail-wind profile is equal to half the magnitude of the head-wind profile, with both profiles being based on climatic data from the primary landing site at Edwards Air Force Base.

The final two profiles represent two of the most severe wind profiles seen to date. The wind profile for STS-2, which flew in November of 1981, consisted of a strong head wind that remained strong to the ground. The fifth profile represents the STS-3 wind profile, which had strong wind shears present. Both the STS-2 and STS-3 profiles have been modified slightly to reflect 500-ft balloon data increments.

The 195-kt normalized touchdown distance for the five wind profiles is listed in Table 1, with all errors being $< \pm 400$ ft. The speedbrake setting at 3000 ft for the ALP and the ASP are shown in Table 2. All errors for the speedbrake calculations are within ± 3 deg, which is acceptable.

As was stated in the introduction, a prime requirement for the ALP is to quickly generate accurate touchdown information to support real-time shuttle operations. On an IBM compatible PC computer with an 80287 math coprocessor, each simulation can be calculated in 25 s.

V. Conclusions

The ALP program provides a quick look approximation of the Shuttle landing conditions, with an accuracy sufficient to support both training and real-time landing operations. Its quick execution time and portability make it suitable for both nominal and emergency operations. All touchdown energy calculations fall within the required 400-ft error allowance of the mainframe-ASP processor. Velocity error calculations on the outer glideslope are within the required 4 kt of the ASP calculations, and the 3000-ft speedbrake setting also satisfies the 3-deg requirement. Thus, the ALP program is expected to augment the mainframe-ASP program effectively during normal Shuttle operations and will also provide a valid computer simulation during emergency situations.

References

[1]Anderson, Jr., D., *Introduction to Flight,* McGraw-Hill, New York, 1978, pp. 52–62.

[2]Anon., "Space Shuttle Operational Level C Functional Subsystem Software Requirements Document, Guidance, Navigation, and Control Part A: Entry Through Landing Guidance," Rockwell International, STS 83-0001B, Downey, CA, June 1987.

[3]Anon., "Operational Aerodynamic Data Book," Rockwell International, STS 85-0118, Downey, CA, Sept. 1985.

[4]James, M. L., Smith, G. M., and Wolford, J. C., *Applied Numerical Methods for Digital Computation,* Harper, New York, 1977, pp. 323–328.

James A. Martin
Associate Editor